UNIVERSITY OF AMSTERDAM

UvA-DARE (Digital Academic Repository)

Engineering retinal-based phototrophy via a complementary photosystem in Synechocystis sp. PCC6803

Chen, Q.

Publication date
2017

Document Version
Other version

License
Other

Link to publication

Citation for published version (APA):
Chen, Q. (2017). *Engineering retinal-based phototrophy via a complementary photosystem in Synechocystis sp. PCC6803*. [Thesis, fully internal, Universiteit van Amsterdam].

General rights
It is not permitted to download or to forward/distribute the text or part of it without the consent of the author(s) and/or copyright holder(s), other than for strictly personal, individual use, unless the work is under an open content license (like Creative Commons).

Disclaimer/Complaints regulations
If you believe that digital publication of certain material infringes any of your rights or (privacy) interests, please let the Library know, stating your reasons. In case of a legitimate complaint, the Library will make the material inaccessible and/or remove it from the website. Please Ask the Library: https://uba.uva.nl/en/contact, or a letter to: Library of the University of Amsterdam, Secretariat, P.O. Box 19185, 1000 GD Amsterdam, The Netherlands. You will be contacted as soon as possible.

UvA-DARE is a service provided by the library of the University of Amsterdam (https://dare.uva.nl)

Download date:16 Mar 2026

Chapter 5

Retinal metabolism in *Synechocystis* sp. PCC6803 and the formation of *holo*-proteorhodopsin

Que Chen, Jeroen B. van der Steen, Aloysius F. Hartog, Srividya Ganapathy, Willem J. de Grip, and Klaas J. Hellingwerf

Abstract:

In many pro- and eukaryotic genera retinal-based proton pumps (*i.e.* rhodopsins) are expressed to equip the cells with the ability of light-driven ATP synthesis, which the cells can use during growth and/or starvation. Such proton pumps also occur in several cyanobacterial genera such as *Gloeobacter violaceus* and *Cyanothece*.

As these retinal-based proton pumps may play an important role in artificially increasing the efficiency of oxygenic photosynthesis (45), it is of interest to characterize retinal metabolism in cyanobacteria. Here we have studied this process in the model cyanobacterium *Synechocystis* sp. PCC6803. It has been proposed, based on the outcome of in *vitro* enzyme activity assays, that two enzymes play a role in retinal synthesis: SynACO and SynDiox2, whereas CYP120A1 has been identified as an enzyme that can hydroxylate the C16, C17 methyl groups of retinal as an initial step in retinal catabolism. Furthermore, the aldehyde retinal may be converted into its corresponding alcohol or carboxylic acid by various more-or-less specific dehydrogenases.

We have studied the in *vivo* role of these five enzyme(s) (activities) presumably involved in retinal metabolism. We confirm the role of SynACO as the decisive enzyme for retinal synthesis in *Synechocystis*, via asymmetric cleavage of β-*apo*-carotenal, while SynDiox2 competes for the same substrates with SynACO, but only measurably contributes to retinal synthesis in the stationary phase via an as yet unknown mechanism. Knocking out the gene encoding SynACO fully abolishes the ability of *Synechocystis* to synthesize retinal. Such mutants can be used for the reconstitution of *holo*-proteorhodopsins with exogenously added retinal or retinal analogues, as we have demonstrated in this study with all-*trans* 3, 4-dehydroretinal and the 3-methylamino-16-nor-1, 2, 3, 4-didehydroretinal analogue.

In *vivo* degradation of retinal can occur through chemical oxidation as well as via physiological pathways. Apparently, in wild-type *Synechocystis*, retinal degradation is faster than retinal biosynthesis, since retinal is only detected in cells expressing *apo*-PR, where it is protected against degradation in *holo*-PR. In the linear growth phase excess *apo*-PR is available, as is evident from quantitation of the cellular levels of retinal and *apo*-PR, an increase of the retinal content is observed in this phase in the knock-out mutant QCSY002 (deletion of gene *slr0574*) also in the late stationary phase. Our results thus suggest that *slr0574* plays a role in the retinal degradation pathway. Prelim-

inary results obtained with [^{13}C]-NMR analysis, however, suggest that also conversion to retinol plays a role.

Key words:

retinal biosynthesis; retinal degradation; retinal analogue; infra-red absorption; retinal supplementation

Introduction

The vastly increasing societal demand for sustainable energy makes it necessary to convert solar energy as efficiently as possible. An important goal in the life sciences, therefore, is to achieve an increase in the energy-conversion efficiency of oxygenic photosynthesis. A widely proposed approach to the latter is by expanding the absorption spectrum of oxygenic photosynthesis into the (far-)red region of the spectrum of electromagnetic radiation (27, 240, 241), as this type of photosynthesis so far is limited to the use of photons in the 350 – 700/750 nm range (17-19). Such an expansion can be achieved by introduction of a heterologous photosystem, like a cyclic electron transfer system of an anoxyphototroph (240, 241) or a retinal-based proton pump (45, 46), provided that these proton-pumping photosystems can exploit far-red photons. The latter approach, *i.e*. the use of a retinal-based proton pump, may be simplest of the two, in terms of requirements in the fields of synthetic biology and physiological adjustment.

Retinal-based photosynthesis is mediated by proton-pumping prokaryotic rhodopsins. These are hepta-helical transmembrane proteins with a covalently bound all-*trans* retinal chromophore (for review see *i.e*. (242)). Our previous study has demonstrated that in *Synechocystis* sp. PCC6803 (hereafter: *Synechocystis*), a model organism for studies of oxygenic photosynthesis, a retinal-based proton pump can contribute measurably to energy conversion for the growth of the organism (46). Remarkably, this study revealed that *Synechocystis* has the capacity to synthesize all-*trans* retinal (46). This brings up the question which biochemical pathway is used for retinal synthesis and -degradation in *Synechocystis*. This topic becomes even more important if one wants to generate transgenic *Synechocystis* strains with a retinal-based proton pump which can utilize far-red light (>700 nm), because this will presumably require – next to the use of retinal analogues (243) – deletion of the endogenous all-*trans* retinal biosynthetic pathway.

Retinal metabolism has been extensively studied, amongst others, in animals, (green) algae, fungi, archaebacteria, and eubacteria. So far, three different pathways have been identified as being involved in retinal biosynthesis, but all via a poly-isoprenoid derived intermediate. Firstly, in animals, a β-carotene-15, 15´-oxygenase (usually abbreviated as 15,15´ BCO or BCO) is commonly employed to generate all-*trans* retinal through symmetrical oxidative cleavage of β-carotene at the C15-C15´ double bond (244, 245). Secondly, halobacteria

use two non-carotenoid oxygenases (the putative membrane protein *Brp* and the *Brp*-like protein *Blh*) to synthesize all-*trans* retinal from β-carotene (246). Thirdly, selected microorganisms utilize *apo*-carotenoids (but not carotenoids) as the precursor of all-*trans* retinal. Examples are the cyanobacteria *Nostoc* sp. PCC7120 and *Fusarium fujikuroi* (247, 248).

Gene sequence comparison shows that in *Synechocystis* two genes have similarity with a carotenoid cleavage dioxygenase (CCD) (249), which are referred to as *sll1541* ((Syn)Diox1, or SynACO), and *slr1648* (SynDiox2), respectively. It has been shown that the enzyme SynACO, in *vitro*, can degrade β-*apo*-carotenals, but not β-carotene, with a wide tolerance with respect to (i) the chain length (*i.e*. between C25 and C35) and (ii) functional end-groups (*i.e*. aldehydes and alcohols; (250). Incubation of the purified SynACO enzyme with carotenoid extracts from *Synechocystis* did not provide convincing evidence on the nature of the physiological substrate nor product of this enzyme in *vivo*. The authors proposed that a C3-hydroxylated *apo*-carotenal with a C27 or C30 chain-length could function as its substrate (250). The crystal structure of SynACO shows that the structure of the substrate-binding pocket of this enzyme is consistent with this substrate specificity (251). The function of SynDiox2 has not been characterized yet, except that it has been claimed that activity of SynDiox2 leads to accumulation of β-13-carotenone (252), which would imply that SynDiox2 functions to cleave β-*apo*-carotenals. Then, with respect to substrate specificity, it would compete with SynACO.

Current knowledge of retinal degradation suggests that retinal in *vivo* is either oxidized into retinoic acid or reduced to retinol. The former reaction is catalyzed by members of the aldehyde dehydrogenase 1 superfamily (ALDH) (253); while the latter reaction can be catalyzed by alcohol dehydrogenase (ADH), retinol dehydrogenase (RDH) and aldo-keto reductase (AKR) (254). Very little information, however, is available with respect to the question which ALDHs and/or ADHs from *Synechocystis* can react with retinoids as their substrate.

Based on gene analysis and substrate specificity identified in in *vitro* assays (255-257), for retinal degradation we decided to specifically investigate in this study the aldehyde dehydrogenase SynAlh1 (encoded by *slr0091*), although in *vitro* assays show that it only oxidizes *apo*-carotenals (chain length ≥ C25) and alkanals, but not retinal, into the corresponding acids (258), and the enzyme AdhA, a medium-chain alcohol dehydrogenase, encoded by *slr1192*, as this enzyme has been shown to be active towards aromatic primary alco-

hols, and preferentially reduces aldehydes rather than oxidiz alcohols (257). Beyond these two enzymes, also the cytochrome P450 enzyme CYP120A1, encoded by *slr0574*, has been included in these studies, as its in *vitro* characterization has led to the suggestion that it accepts not only retinoic acid, but also retinal as a substrate and is able to introduce a single hydroxyl group at the C16 or C17 position of this latter substrate (252).

In conclusion, in the present study, we have characterized the role of *sll1541* and *slr1648* in retinal synthesis, and *slr0091*, *slr0574*, and *slr1192* in retinal degradation in *Synechocystis*. We show that SynACO is an indispensable enzyme for retinal synthesis, while SynDiox2 seems to convert the same substrate(s) (*i.e*. *apo*-carotenoids) as SynACO, but presumably into a wider range of products than only retinal. SynDiox2, however, may be important for retinal biosynthesis in the late- or stationary phase of growth. As for retinal degradation, we show that *slr0574* plays a crucial role in the retinal catabolic pathway.

Moreover, we also show reconstitution of *apo*-PR, expressed in a retinal-free *Synechocystis* strain, upon supplementation with retinal analogues into *holo*-proteorhodopsin. This paves the way to generate PR-expressing strains that can harvest infra-red light (>700 nm,) by supplementing the cyanobacterium with a strongly red-shifting retinal analogue.

Materials & Methods

Strains and growth conditions

Strains of *Escherichia coli* were routinely grown in LB-Lennox (LB) liquid medium at 37°C with shaking at 200 rpm, or on solid LB plates containing 1.5% (w/v) agar.

Synechocystis sp. PCC6803 (a glucose tolerant strain, obtained from D. Bhaya, Stanford University, USA) was routinely grown at 30°C with continuous illumination by white light at moderate intensities of approximately 45 µmol • m^{-2} • s^{-1} (= µmol photons • m^{-2} • s^{-1}). Liquid cultures were grown in BG-11 medium (Sigma-Aldrich), supplemented with 50 mM sodium bicarbonate, 25 mM TES-KOH (pH 8) and appropriate antibiotics, and with shaking at 120 rpm (Innova 43, New Brunswick Scientific). The BG-11 agar plates were supplemented with 10 mM TES-KOH (pH= 8), 5 mM glucose, 20 mM sodium thiosulfate, and 1.5% (w/v) agar.

Where appropriate, antibiotics were added to the following final concentration: ampicillin (100 µg/ml), kanamycin (25 to 50 µg/ml), chloramphenicol (35 µg/ml), streptomycin (10 µg/ml), and spectinomycin (25 µg/ml), either separately or in combination.

Strain construction

Genomic sequences of *sll1541*, *slr1648*, *slr0091*, *slr0574* and *slr1192*, which encode SynACO, SynDiox2, SynAlh1, CYP120A1, and AdhA, respectively, where derived from CyanoBase (259). Unless noted otherwise, PCRs were performed with the proofreading Pwo DNA Polymerase (Roche Diagnostics) or the Herculase II fusion enzyme (Agilent Technologies). Plates were incubated under low-intensity continuous illumination in a humidified incubator.

Null mutants of *sll1541* (strain JBS14001) were constructed by double-homologous recombination with a fusion PCR product consisting of three fragments: a fragment of approximately 1400 bps adjacent to *sll1541* (hom1), a fragment containing an omega antibiotic-resistance cassette, and a fragment of approximately 1400 bps adjacent to the complementary side of *sll1541* (hom2). The hom1 and hom2 fragments were amplified from genomic DNA with primers JBS391 & JBS392, and JBS395 & JBS396, respectively, which introduced overlaps with the omega fragment. The omega fragment was amplified from pAVO-cTM1254 (260) with primers JBS393 & JBS394, which introduced overlaps with both the hom1 and the hom2 fragment. The three fragments were fused together in a PCR of 15 cycles without additional primers, after which primers and extra dNTPs were added and the PCR was continued for an additional 25 cycles.

Null mutants of *slr1648* (strain JBS14002) were constructed using the same approach, except that a chloramphenicol resistance cassette was used as the marker. Primers JBS397 and JBS398, and JBS401 and JBS402 were used to amplify the corresponding hom1 and hom2 fragment from genomic DNA. Primers JBS399 & 400 were used to amplify the chloramphenicol resistance cassette from plasmid phaAHCmH (261).

The resulting fragments were gel-purified using the QIAGEN QIAquick Gel Extraction Kit (QIAGEN) or the Bioline ISOLATE II PCR and Gel Kit (Bioline) according to the instructions provided by the manufacturers.

Null mutants of *slr0091* (strain QCSY001) were constructed by double-homologous recombination with a plasmid pQC016, that derived from plasmid pWD013 containing the omega antibiotic-resistance cassette. For pWD013 plasmid construction, upstream (hom1) and downstream (hom2) homologous regions (approximately 1000 bps each) of *slr0091* were amplified from *Synechocystis* genomic DNA with primers Adh-up-Fwd / Adh-up-Rev and Adh-down-Fwd / Adh-down-Rev, respectively. Those primers also introduce overlaps between hom1 and hom2, and thus the generated fragments were fused together with Pfu DNA Polymerase (Thermo Scientific). After gel extraction and purification (Zymo Research), an extra adenosine ("A") was added as the 3' overhang of the fusion fragment, using Taq DNA Polymerase (Thermo Scientific). Then, this fragment was ligated to the BioBrick "T" vector pFL-SN (262). The omega antibiotic-resistance cassette, amplified with primers QC37/QC38, was inserted between hom1 and hom2 of plasmid pWD013, using the XbaI restriction enzyme.

A null mutant of *slr0574* (strain QCSY002) was constructed by double-homologous recombination with plasmid pQC015, carrying three fragments: A fragment of approximately 1000 bps adjacent to *slr0574* (hom1), a chloramphenicol resistance cassette, and a fragment of approximately 1000 bps adjacent to the complementary side of *slr0574* (hom2). Hom1 and hom2 were amplified from genomic DNA by primers QC43/QC44, and QC47/QC48, respectively, and then introduced into plasmid PFL-XN/Cm (+) (262), which contains a chloramphenicol resistance cassette, by plasmid restriction with the enzymes NheI /PstI and XbaI, respectively.

Genome segregation

For transformations with mutagenic plasmids and linear DNA fragments, *Synechocystis* sp. PCC6803 was grown until an OD_{730} (optical density at 730 nm) of 0.2 to 0.3. Cells were then concentrated by centrifugation to an OD_{730} of 2.5 in a volume of 100 µl of fresh BG-11 plus 20 mM TES-KOH (pH 8.0) in a sterile 1.5 ml Eppendorf cup. To this, a maximum of 10 µl of purified fusion PCR product or 1 µg of plasmid DNA was added. The mixture was incubated at 30°C in the light in a shaking incubator (regular growth conditions) for 5 to 8 h. Cells were then incubated on BG-11 plates containing 10 mM TES-KOH (pH 8.0), 5 mM glucose and 20 mM sodium thiosulfate, and supplemented with the corresponding antibiotic(s) at a low concentration. Single colonies were next plated on plates containing increasingly higher concentrations of antibiotic to promote genome segregation. The final concentrations of the antibiot-

ics used were: a mix of 25 µg/ml spectinomycin and 10 µg/ml streptomycin for the *sll1541* mutant and the *slr0091* mutant, 65 µg/ml chloramphenicol for the *slr1648* mutant and the *slr0574* mutant, and 20 µg/ml Zeocin for the *slr1192* (deletion) mutants. Full segregation for all these strains was confirmed with PCR tests using MyTAQ polymerase (Bioline) with flanking primers JBS391 and JBS396 for Δ*sll1541*, JBS397 and JBS402 for Δ*slr1648*, Adh-up-Fwd and Adh-down-Rev for Δ*slr0091*, QC43 and QC48 for Δ*slr0574*.

The double null mutants of *sll1541* and *slr1648* (strain JBS14003) and of *slr0091* and *slr0574* (strain QCSY003) were created by transforming the segregated single mutants with the appropriate fusion PCR product or plasmid, using an identical protocol as described above. After full segregation, the continued presence of the first null mutation was confirmed by PCR as well.

Conjugation

The relevant strains were conjugated with plasmid pQC006 (46) (encoding His-PR) or plasmid pJBS1312 (46) (empty-plasmid control) as described in (46). The presence of the plasmids and the continued presence of the null mutations of *sll1541*, *slr1648*, *slr0091*, *slr0574* and *slr1192* were confirmed with appropriate PCR tests after the conjugation procedure.

Retinal identification and quantification

To investigate the retinal content of selected mutants, and its dependence on the cellular growth phase, batch cultures were grown under the same conditions (see growth conditions, above) and cells were removed at different growth phases for retinal quantification. Retinal was isolated, identified and quantified essentially as described before (46). In short, cell pellets were first processed to react with hydroxylamine so as to convert retinal to the more stable compound retinal oxime (233). The obtained extract was separated on an HPLC system with an EC 150/4.6 NUCLEOSIL 100-5 C18 column (MACHEREY-NAGEL), and n-heptane (HPLC grade) at 1 ml/min as the mobile phase. The retinal content was determined by the peak area of the oxime form of retinal, and compared with that of a series of known amounts of retinal (oxime).

To precisely quantify retinal A1 (all-*trans* retinal) and retinal A2 (all-*trans* 3,4-dehydroretinal) in a sample, the peak area was integrated at 354.2 nm and 367.8 nm, respectively, where the oxime forms of retinal A1 and A2 maxi-

mally absorb. Quantitative analysis of the molar ratio of retinal A1 and A2 in a sample, or in a mixture, was calculated based on the peak areas and the extinction coefficients of A1 and A2, taken as 49,000 and 44,000 $M^{-1} \cdot cm^{-1}$, respectively (265, 266).

To present retinal production in units of the number of retinal molecules per cell, the number of cells was estimated on basis of the conversion factor that 1 ml culture of wild-type *Synechocystis* with an OD_{730} = 1 contains 10^8 cells, as determined with a Casy 1 TTC cell counter (Schärfe System GmbH, Reutlingen, Germany) (232).

Isolation of His-tagged proteo-opsin from *Synechocystis*

His-tagged protein from *Synechocystis* cells was isolated and purified by using a HisTrap FF Crude column with 5 ml column volume, and an ÄKTA FPLC system (all from GE Healthcare, Uppsala, Sweden). Cell pellets were disrupted by use of a bead beater and the purification procedure essentially followed the protocol described in (46).

When necessary, all-*trans* retinal or the retinal analog (all-*trans* 3,4-dehydroretinal (retinal A2) or 3-methyl-amino-16-nor-1,2,3,4-didehydroretinal (MMAR)) was added in a solution of ethanol, separately or in combination, to the culture at the final concentration of 20 µM, when cell density of culture (OD_{730}) had reached approximately 2. Then, retinal or the retinal analog was added every 24 hours for two consecutive days.

Table 1: Strains or plasmids constructed for this study

Strain or plasmid	Relevant characteristics[a]	Source or reference
Strains		
Synechocystis sp. PCC6803		
WT	A glucose tolerant *Synechocystis* sp. PCC6803	fromD.Bhaya, Stanford University, Stanford, CA
JBS14001	Spc^R, Str^R; Δ*sll1541*:: Ω^R; chromosomal deletion of gene *sll1541*	This study
JBS14002	Cam^R; Δ*slr1648*:: Cm^R; chromosomal deletion of gene *slr1648*	This study
JBS14003	Spc^R, Str^R, Cam^R; Δ*sll1541*:: Ω^R , Δ*slr1648*:: Cm^R; chromosomal deletion of gene *sll1541* and *slr1648*	This study
QCSY001	Spc^R, Str^R; Δ*slr0091*:: Ω^R; chromosomal deletion of gene *slr0091*	This study
QCSY002	Cam^R; Δ*slr0574*:: Cm^R; chromosomal deletion of gene *slr0574*	This study
QCSY003	Spc^R, Str^R, Cam^R; Δ*slr0091*:: Ω^R, Δ*slr0574*:: Cm^R; chromosomal deletion of gene *slr0091* and *slr0574*	This study
UL025	Zoe^R; Δ*slr1192*:: Zoe^R, chromosomal deletion of gene *slr1192*	A kind gift from Prof. T. Pembroke, Limerick, Ireland
Escherichia coli		
XL1-Blue	Cloning host	Agilent Technologies
J53/RP4	Helper strain	(263, 264);
Plasmids		
pJBS1312	kan^R; expression vector, pVZ321 origin, P_{psbA2}	(46)
pQC006	kan^R; pJBS1312-based expression of pR, C-terminal 6×histine tagged	(46)
pFL-SN	Amp^R, Cm^R; BioBrick "T" vector with XcmI on each side	(262)
pFL-XN	Amp^R, Cm^R; BioBrick "T" vector with SpeI and NheI and XbaI on one side of chloramphenicol cassette	(262)
pWD013	pFL-SN derivate, Amp^r, containing upstream and downstream homologous regions of the *slr0091* gene	This study
pQC016	pFL-SN derivate, Amp^R, Spc^R, Str^R; containing *slr0091* gene upstream and downstream homologous regions and a Ω resistance cassette in between	This study
pQC015	pFL-SN derivate, Amp^R, Cm^R; containing *slr0574* gene upstream and downstream homologous regions and a chloramphenicol resistance cassette in between	This study

[a] Ω is short for the omega resistance cassette; Cm^R represents the chloramphenicol resistance; while Amp^R means the ampicillin resistance cassette; Kan^R for kanamycin resistance; Zoe^R for the zeocin resistance; Spc^R for spectinomycin resistance and Str^R for streptomycin resistance.

Results

Retinal synthesis in *Synechocystis*

Two genes, *i.e*. *sll1541* (encoding SynACO) and *slr1648* (SynDiox2), have so far been identified as a carotenoid cleavage dioxygenase (CCD) in *Synechocystis* (249). In *vitro* assays have shown that the product of both genes can convert β-*apo*-carotenals, but with different products as a result (see also Fig. 1): all-*trans* retinal for SynACO (250) and β-13-carotenone for (SynDiox2 (252). However, due its rapid catabolism and limited in *vivo* stability, significant amounts of retinal were not detected in *Synechocystis* until recently. This situation changed after heterologous expression of a microbial rhodopsin in this cyanobacterium (*i.e*. a proteorhodopsin; hereafter: PR). It was observed that this allows the *apo*-form of PR to bind and protect all-*trans* retinal so that it can accumulate as the bound chromophore of *holo*-PR in the cells (45, 46).

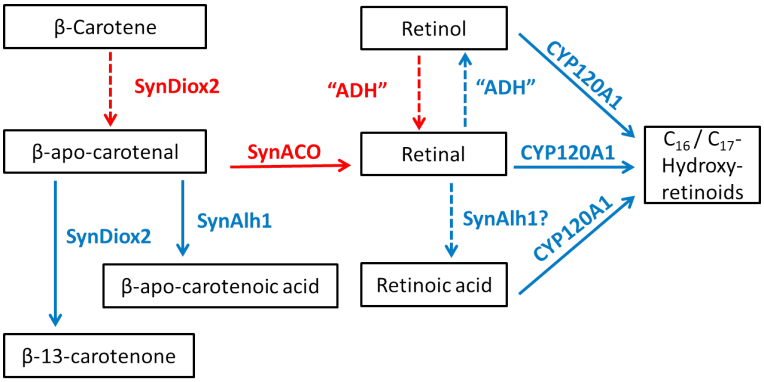

Figure 1: Tentative scheme of retinal synthesis and degradation in *Synechocystis*. Summarizing available information from in *vitro* obtained data from the literature (250, 252, 257, 267). Solid arrows represent reactions that have been demonstrated in *vitro*, while dotted lines represent hypothetical pathways in *Synechocystis*. Moreover, the pathways in red and blue represent the presumed pathways for synthesis and degradation of retinal in *vivo*.

Based on the availability of the *apo*-PR expression system, as well as the knowledge from in the in *vitro* analyses, we have designed experiments to elucidate the pathway of retinal biosynthesis and degradation in *Synechocystis* cells in *vivo*. Accordingly, we first concentrated on the role of *sll1541* and *slr1648* in retinal synthesis. Our strategy was to quantify retinal content in various mutants, all containing plasmid pQC006 (which drives high-level expression of histidine-tagged *apo*-PR; (46)). These mutants additionally would carry

a deletion in one or both of the above genes (*i.e*. *sll1541* and/or *slr1648*) introduced through natural–transformation based deletion mutagenesis. The resulting strains are referred to as: JBS14001, JBS14002, and JBS14003. Wild-type *Synechocystis* carrying plasmid pQC006 is the positive control in these experiments. To explore the effect of deletion of these genes on the growth of *Synechocystis*, batch cultures were grown at a moderate light intensity (~ 45 µmol • m^{-2} • s^{-1}) in BG-11 medium, supplemented with the antibiotic for plasmid maintenance (see Materials and Methods). Fig. 2A shows that, under our conditions, no significant difference in growth rate was observed between the wild-type control and the three mutants, be it that mutants JBS14001 and JBS14003 show a slightly higher final OD than the wild type.

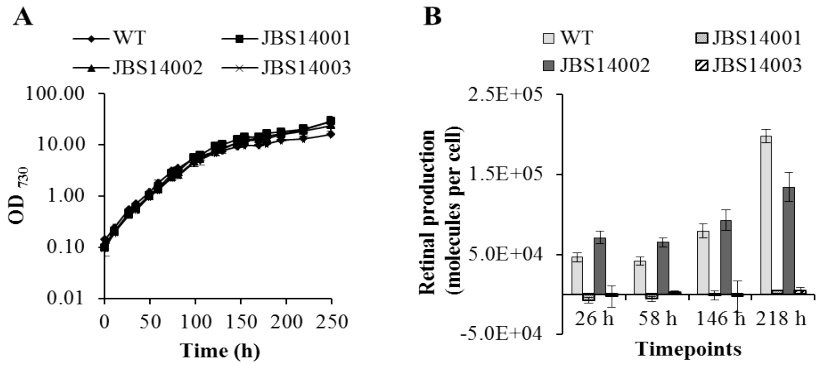

Figure 2: All-*trans* retinal production in four *Synechocystis* strains grown in batch culture as a function of growth phase. Cells were grown in the BG-11 medium at the moderate light intensity. A) Growth curves monitored via the OD_{730} for comparison of the wild type strain with deletion strains in *sll1541* (JBS14001), *slr1648* (JBS14002) and *sll1541* plus *slr1648* (JBS14003). Gene *sll1541* and *slr1648* encodes enzyme SynACO and SynDiox2, respectively. All strains were conjugated with plasmid pQC006 (for PR-His expression). Error bars represent the standard deviation of 3 biological replicates (n=3) and are only visible when they exceed the size of the symbols. B) all-*trans* retinal production, expressed in a bar graph as the number of all-*trans* retinal molecules per cell. Samples were taken at 26 h, 58 h, 146 h, and 218 h for all-*trans* retinal quantification by HPLC analysis. Error bars represent the standard deviation of 5 replicates.

From such experiments, cells were harvested at various time points to reveal the dependency of the retinal content on the growth phase of *Synechocystis*. After harvesting the cells, their retinal content was quantified by means of HPLC analysis (46). These results revealed that no retinal could be detected in the mutants JBS14001 and JBS14003, both of which carry a deletion of *sll1541* (encoding SynACO). In contrast, strain JBS14002, carrying a deletion of *slr1648* (encoding SynDiox2), had a slightly higher retinal content than the wild type, in both the exponential phase and in the linear growth phase

(represented by the samples taken after 26 h and 58 h, respectively), but still one-third less than wild type in the late stationary phase (*i.e*. after 218 h). These results strongly suggest that *sll1541* plays the decisive role in retinal synthesis in *Synechocystis*; while SynDiox2 presumably consumes the same precursor(s) as SynACO, to convert these substrates into products other than all-*trans* retinal.

The typical growth-phase dependency of the retinal content observable in Fig. 2B in both the wild type and in JBS14002, *i.e*. that retinal levels dropped slightly during the linear phase of growth (at the 58 h time point), and then increased as cells gradually enter stationary phase, has been observed repeatedly. Significantly, in the wild-type strain, a sharp increase in retinal content was seen in the late stationary phase. Particularly *slr1648* (SynDiox2) is probably important for this phase of retinal production (Fig. 2B).

Purification of histidine-tagged Proteorhodopsin from a mutant strain deficient in retinal synthesis

As the data presented in Fig. 2B clearly show that mutants with a deletion of *sll1541* lose the ability to produce all-*trans* retinal, this allows for experiments with the aim of altering the chromophore of *holo*-PR in *vivo*. The success of this approach can easily be traced because of the typical property of the native *holo*-PR, *i.e*. the main absorption band with a maximum at 516 nm under slightly alkaline conditions. The corresponding experiment was carried out with strain JBS14003 (carrying a deletion in *sll1541* and *slr1648*) containing plasmid pQC006 (for *apo*-PR-His expression). Cultures were grown under a mixture of red and blue light at a moderate combined light intensity (~ 35 µmol • m^{-2} • s^{-1} , with or without exogenous addition of 10 µM all-*trans* retinal. Wild-type *Synechocystis* conjugated with plasmid pQC006, as a control strain, was grown under the same conditions, but without the addition of all-*trans* retinal. His-tagged proteorhodopsin was purified from harvested cells as described before (see Materials and Methods) and the UV/visible absorption spectrum of the eluted fractions was recorded by spectrophotometry.

As expected, the relevant fractions from the control strain (*Synechocystis* wild type (WT) + pQC006) showed a pink appearance (data not shown), and their spectra contained an absorption peak in the range of 400 to 600 nm, with a maximum at 516 nm (Fig. 3, dotted curve). These characteristics clearly suggest the presence of significant amounts of *holo*-PR. Significantly, none of these characteristics was observed for the corresponding fractions from the

strain JBS14003, containing plasmid pQC006 (Fig. 3, solid curve). Furthermore, when this mutant JBS14003 (plus pQC006) is supplied with exogenous all-*trans* retinal, as shown in Fig. 3 (dashed curve), the relevant eluted fractions do show the typical absorption spectrum of *holo*-proteorhodopsin. This leads us to conclude that *sll1541* is indispensable for retinal synthesis in *Synechocystis* sp. PCC6803: Deletion of *sll1541* completely halted the synthesis of all-*trans* retinal and subsequent formation of *holo*-PR. The peaks in these spectra in the range of 350 to 450 nm and 650 to 700 nm that consistently showed up in PR-containing fractions obtained from *Synechocystis*, show that small amounts of (presumably protein-bound) chlorophyll a (and possibly carotenoids) are present in these samples.

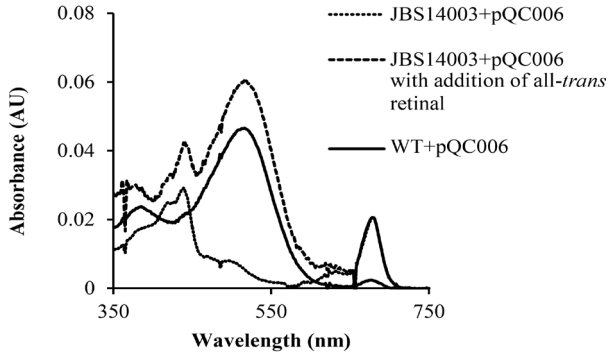

Figure 3: Spectra eluted from a Ni3+-affinity column for purification of His-tagged proteorhodopsin from *Synechocystis*. A strain deficient in retinal synthesis (JBS14003, with a deletion in *sll1541* and *slr1648*), conjugated with plasmid pQC006 (for the expression of PR-His), was cultivated in BG-11 medium, supplemented with or without 10 µM all-*trans* retinal. Wild-type *Synechocystis* conjugated with plasmid pQC006 was used as the positive control.

Reconstitution of *apo*-PR with a red-shifted retinal analogue in *vivo*

The previous experiment has shown that it is possible to regenerate *holo*-proteorhodopsin in *Synechocystis* cells by incubating a retinal chromophore together with *apo*-PR in a strain deficient in retinal synthesis (*i.e*. JBS14003 + pQC006). Because of our interest in a red-shifted, and retinal-based proton pump in *Synechocystis* (45), we selected the retinal analogue MMAR (Fig. 4), which was shown to red-shift the absorbance band of PR by about 50 nm relative to native retinal, with additional tailing out to about 850 nm (229). Thus we supplemented a *Synechocystis* batch culture with MMAR for reconstitution of *apo*-PR in intact cells of JBS14003 + pQC006.

The UV/Vis absorption spectrum of His-tagged proteorhodopsin, reconstituted with MMAR purified from *Synechocystis*, shows a main broad absorption peak with a maximum at 570 nm, and a low-energy shoulder from 700 to ~ 850 nm. This is the first time that a photo-active protein has been isolated from *Synechocystis* which can absorb light of wavelengths beyond 750 nm. This spectrum also reveals the presence of traces of contaminating chlorophyll (see also above). The absorption of these contaminants overlaps with our protein of interest in the range of 650-700 nm. In order to record a precise spectrum of PR from *Synechocystis* reconstituted with MMAR, we subtracted the spectrum of the *apo*-PR-His fraction from *Synechocystis* (from strain JBS14003 + pQC006). The spectrum of MMAR-reconstituted PR, isolated from *E. coli*, served as the positive control. Based on this, we conclude that the main absorbance band of these two proteorhodopsin analogues (*i.e*. isolated from *Synechocystis* and *E. coli*) is factually identical (Fig. 4B). The difference in the strength of the 280 nm band may be due to the correction procedure or to differences in the level of contamination with *apo*-protein and/or host proteins. These results also demonstrate that this MMAR retinal analogue is not metabolically modified prior to incorporation into PR.

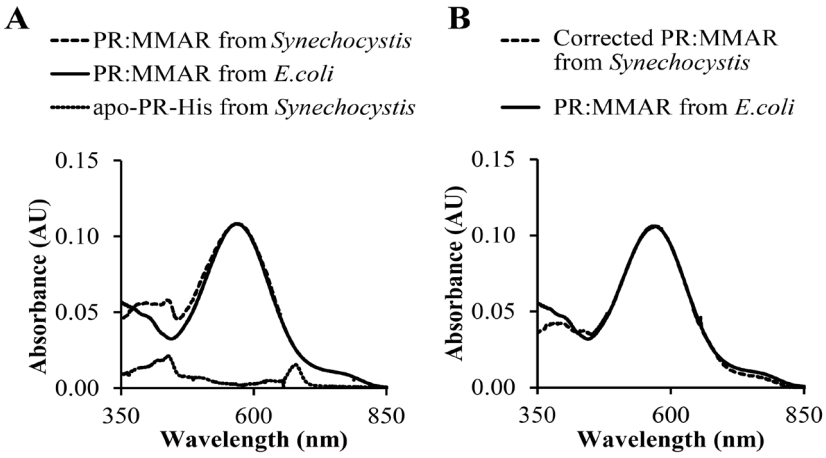

Figure 4: Incorporation of a retinal analogue in *apo*-proteorhodopsin in *vivo*. A strain deficient in retinal synthesis, JBS14003, conjugated with plasmid pQC006 (for expression of PR-His), was inoculated in BG-11 medium, with or without exogenous addition of the retinal analogue MMAR (chemical structure on top). Spectra were normalized on the 570 nm absorbance. A) MMAR-containing PR-His purified from *Synechocystis*; MMAR-containing PR-His purified from *E. coli*; and *apo*-PR-His purified from *Synechocystis* (for the explanation of the symbols: see inset in the figure). B) The corrected spectrum of MMAR-containing PR purified from *Synechocystis* and from *E. coli*.

Binding affinity of *apo*-PR for retinal A1 and retinal A2 in *Synechocystis*

We exploited the fact that PR has binding affinity for both retinal A1 and all-*trans* 3,4-dehydroretinal (retinal A2) (Ganapathy et al., 2015) to investigate the relative affinity of *apo*-PR in *Synechocystis* for these two chromophores. Hereto, we utilized two mixtures with different ratios of A1 and A2 as the substrate for in *vivo* reconstitution. HPLC analysis of both mixtures, after their conversion to the oxime form (with hydroxylamine), showed that both samples contained two fractions, eluting at 2.85 min and 3.17 min, respectively (Fig. 5A). On the basis of their spectra, these two components have been identified as the oxime-form of A1 and A2, respectively (Foster et al., 1993). Quantitative analysis, on the basis of peak area and the respective extinction coefficient, suggests that their molar ratio in these mixtures is: A1: A2 = (25.4 ± 3.8): (74.6 ± 3.8) and (15.2 ± 0.31): (84.8 ± 0.31), respectively.

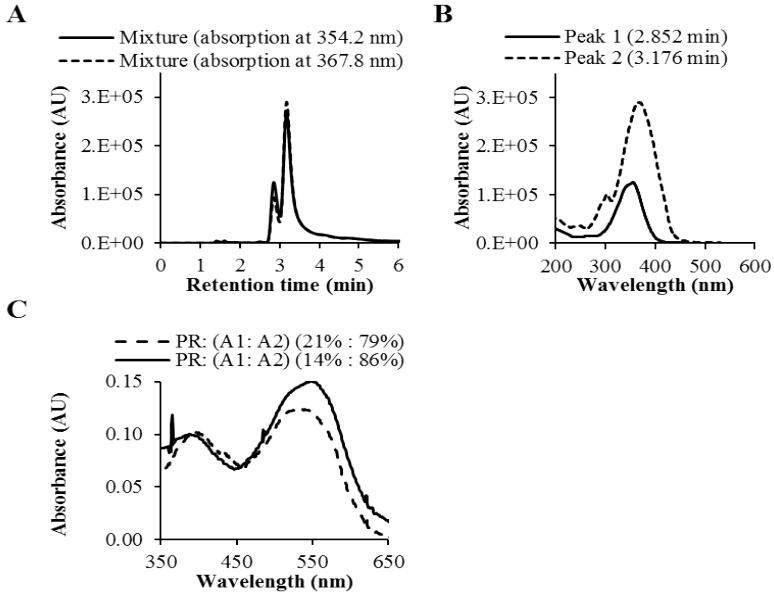

Figure 5: Analysis of the binding specificity of apo-PR for retinal A1 and A2 in Synechocystis. A) Elution pattern of the two chromophores from the HPLC system as measured via the absorption at 354.2 nm (solid line) and 367.8 nm (dashed line) —the absorbance maxima of the oxime form of retinal A1 and A2, respectively. B) The absorption spectrum of the two peaks separated by HPLC, which confirms that the compound eluting at 2.852 min is the oxime form of retinal A1 (solid line), while the compound eluting at 3.176 min is the oxime form of retinal A2 (dotted line). C) Incorporation of a mixture of retinal A1 and A2 into *apo*-proteorhodopsin in *Synechocystis* in *vivo*. A retinal-synthesis deficient strain, JBS14003, conjugated with plasmid pQC006 (for expression of PR-His), was inoculated with a mixture at a different molar ratio of all-*trans* retinal A1 and all-*trans* retinal A2. *Holo*-PR was then isolated from *Synechocystis*.

We supplemented the above two mixtures of retinal A1 and A2 with *apo*-PR in two separate cultures of *Synechocystis* (JBS14003+ pQC006). Upon isolation of the reconstituted and purified *holo*-PR-His, both samples showed an absorption peak with a maximum at 560 nm, but with a shoulder at 518 nm. This confirmed the binding of both retinal A2 and A1 to *apo*-PR-His. The ratio of the absorption maxima at 518 nm and 560 nm varied depending on the composition of the retinal mixture provided to the cells. HPLC analysis of chromophores re-isolated from the purified *holo*-PR-His samples from these cells showed that the chromophore composition (*i.e*. the ratio of retinal A1 over A2) of (21.5 ± 1.4) : (78.5 ± 1.5) and (16.1 ± 0.19) : (83.9 ± 0.19) of these protein samples is very similar to the chromophore ratio's used for the in *vivo* reconstitution (see above paragraph). We therefore conclude that *apo*-PR has about the same affinity for these two chromophores and that the specificity of their binding does not change when PR is expressed in *Synechocystis*, while in the latter organism a significant part (*i.e*. about 50%; (46)) of the protein is embedded in the thylakoid membrane.

Retinal degradation in *Synechocystis*

Our previous study proved that *Synechocystis* has the ability to synthesize all-*trans* retinal, but apparently also rapidly degrades it because retinal cannot be detected in *Synechocystis* cells unless these cells heterologously express a proteorhodopsin. This indicates that *Synechocystis* may have developed (a) system(s) to efficiently degrade retinal. Current literature suggests that retinal degradation in *vivo* is mainly initiated either by enzymes from the aldehyde dehydrogenase 1 superfamily (ALDH) (253) into retinoic acid, or by an alcohol dehydrogenase (ADH), a retinol dehydrogenase (RDH) and/or an aldo-keto reductase (AKR) (254) into retinol. *Synechocystis* has several members in both the ALDH family and the ADH family, but no information was available so far in the literature with respect to how effectively ALDHs or ADHs in *Synechocystis* would convert retinoids like retinal.

To explore retinal catabolism in *Synechocystis* in *vivo*, we decided to investigate the role of ALDHs, ADHs, and CYP450s in retinal degradation by knocking out the relevant genes. Based on gene analysis and substrate specificity identified in *vitro* assays (255-257), the most promising candidates for this part of our study are aldehyde dehydrogenase SynAlh1, encoded by *slr0091*, a medium-chain alcohol dehydrogenase (AdhA), encoded by *slr1192* and the cytochrome P450 isoform CYP120A1, encoded by *slr0574*.

With an attempt to see a significant increase in retinal content after deleting relevant genes, we first quantified the retinal content in mutants with a deletion of one or more of the above genes (*i.e*. *slr0091*, *slr0574*, *slr0091* and *slr0574*, and *slr1192*, in the following referred to as strain QCSY001; QCSY002; QCSY003 and UL025; see also Table 1), while wild-type *Synechocystis* was taken as the control. However, although we took samples at four different growth phases from the culture of each strain, no retinal was detected in any of the mutants, or in WT, at any growth phase. This result is consistent with our previous observation that, in *Synechocystis*, heterologous expression of proteorhodopsin is strictly required for the protection of retinal against degradation.

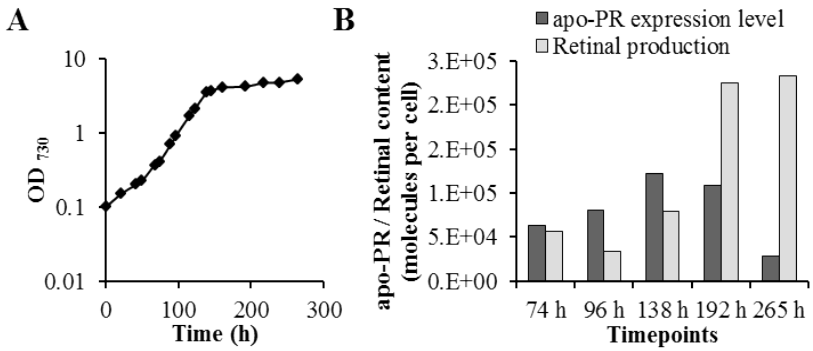

Figure 6: Cellular retinal content in batch cultures of a PR-expressing *Synechocystis* strain as a function of the growth phase of the culture. Cells were grown in the BG-11 medium at the moderate light intensity. A) Growth curve of the wild type, conjugated with plasmid pQC006 (for PR-His expression), and monitored via the OD_{730}. B) all-*trans* retinal content and *apo*-PR expression level as a function of growth phase in wild-type + pQC006. Both are expressed as bars in units of the number of molecules per cell. Samples were taken after 74 h, 96 h, 138 h, 192 h, and 265 h for all-*trans* retinal quantification by HPLC analysis and for (*apo*-)PR-His quantification via Western blots. The data shown are from a representative experiment.

For that purpose, we conjugated our PR-expression plasmid pQC006 into all the above mentioned retinal degradation deletion mutants. As retinal is chemically rather unstable, particularly in the light, retinal accumulation due to disruption of degradation can be visible only when a significant fraction of *apo*-PR is existing in cells, so that *apo*-PR can stabilize retinal and make it detectable. Our previous study showed that both the *apo*-PR expression level and the retinal content in WT, conjugated with pQC006, changes during the subsequent growth phases (46), hence a time window has to be identified in which the *apo*-PR level is relatively high.

Fig. 6B shows a clear difference in the retinal content and level of *apo*-PR expression as growth progresses in WT + pQC006. The level of *apo*-PR expression continuously increased and reached a peak in the early stationary phase, followed by a continuous decrease. In parallel, the retinal content showed an overall increasing trend, but with a significant decrease at the start of the linear growth phase. By calculating the molar ratio of apo-PR to retinal, we found, among those five sampling points, that the highest ratio of *apo*-PR to retinal was present in the linear growth phase. Two independent biological experiments yielded a molar ratio *apo*-PR/retinal in that growth phase of 1.9 and 2.3. Therefore, we concluded that a time point in the linear growth phase provides a suitable time window to monitor a potential increase in retinal content in mutants impaired in their ability to degrade retinal. Beyond that, the late stationary phase also may be informative in this respect, as in this growth phase a high retinal content is consistently detected in WT+pQC006. Hence, this could also be a time window, where any effect of the null mutations could become apparent.

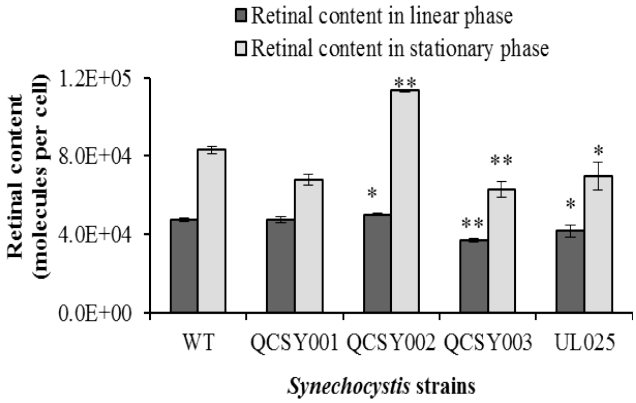

Figure 7: Comparison of the retinal content of the wild type and of four *Synechocystis* deletion strains: *slr0091* (QCSY001); *slr0574* (QCSY002); *slr0091* plus *slr0574* (QCSY003); and *slr1192* (UL025). Gene *slr0091*, *slr0574* and *slr1192* encode the enzymes SynAlh1, CYP120A1 and AdhA, respectively. All strains were conjugated with plasmid pQC006 (for PR-His expression). Samples were taken in the linear growth phase (OD_{730} ~ 0.95) and in the stationary phase (OD_{730} between ~3 and 4), for all-*trans* retinal quantification by HPLC analysis. Error bars represent the standard deviation of 4 replicates. Statistical significant differences to the strain WT are marked by an asterisk. The significance is indicated by stars: ** for a p-value < 0.001, and *for p-value < 0.05.

The retinal-degradation experiment was performed with five *Synechocystis* strains, carrying a deletion of gene *slr0091* (encoding SynAlh1; strain QCSY001); *slr0574* (encoding CYP120A; QCSY002); *slr0091* and *slr0574* (encoding SynAlh1 and CYP120A, respectively; QCSY003); or *slr1192* (en-

coding AdhA; UL025), and the wild-type served as the control. All these strains were conjugated with plasmid pQC006 (for PR-His expression). From each culture, a batch of cells was harvested in the linear growth phase (OD_{730} ~ 0.95) and in the stationary phase (OD_{730} between 3 and 4) for all-*trans* retinal quantification. HPLC analysis of those samples shows that the retinal content of QCSY002 + pQC006 was higher than that of the WT + pQC006 in both linear growth phase and stationary phase (Fig. 7), which implies that the product of gene *slr0574* is involved in retinal degradation.

Discussion

Retinoids (in particular retinal, retinol, and retinoic acid) are critical molecules for most forms of life with respect to vision, normal embryonic development, and for control of cellular growth, differentiation, energetics and death (242, 268, 269). Sequence alignment shows that genes with significant similarity to BCO I/BCO II (β-carotene-cleaving enzymes) are widely spread among the cyanobacteria (250, 270). Consistent with that, studies on cyanobacterial blooms in eutrophic lakes have revealed that retinal was widely detected in many of the 39 species of freshwater cyanobacteria and algae identified (271). Beyond that, earlier findings on the occurrence of retinylidene receptors in Calothrix (272); Anabena (273) Leptolyngbya (274); *Nostoc* sp. PCC7120 (275) and *Gloeobacter violaceus* PCC 7421 (276) confirmed the widespread occurrence of retinoids in cyanobacteria.

However, relatively little information on retinoid metabolism (and biological function; but see *i.e*. (273)) was documented for members of the cyanobacteria, although the characteristics of relevant enzymes from *Nostoc* sp. PCC7120 and Synechosystis sp. PCC6803 have been extensively investigated in *vitro*. Therefore, we have initiated a study to elucidate the metabolism of retinal in *vivo* in the model cyanobacterium *Synechocystis* sp. PCC6803, to start filling this gap and pave the way for further studies of retinoid metabolism and function in (engineered) cyanobacteria.

Our investigation on retinal synthesis shows that deletion of *sll1541* (encoding SynACO) completely impaired the ability of the cells to synthesize all-*trans* retinal in *Synechocystis*, which suggests that SynACO is decisively involved in retinal synthesis. This result confirmed its enzymatic activity identified in *vitro*. Beyond that, we also observed that deletion of *slr1648* (encoding SynDiox2) resulted in a considerable stimulation of retinal production during early growth stages. Enzymatic characterization of the activity of SynDiox2 has led to the

claim that its activity leads to the accumulation of β-13-carotenone. A subsequent study on NSC3 (also named NosDiox2, a homologue of SynDiox2) proved that NSC3 also consumes β-*apo*-carotenal, but cleaves it at the C-13 C-14 or C-13' C-14' double bond, so that it synthesizes β-*apo*-carotenone (277). Together with our data, this implies that SynDiox2 in Synechocytis actually competes with SynACO for the same substrates, so that deletion of *slr1648* can drive more flux through SynACO, to produce more retinal. Strikingly, the study on NSC3 revealed a new cleavage position at the C15-C15' double bond with certain substrates (277). However, no retinal was found in our strain JBS14001 + pQC006, the mutant in which SynACO had been deleted but SynDiox2 is still present. This enzyme, therefore, did not measurably cleave carotenoids at the C15 C15' double bond, which would have directly generated retinal in *Synechocystis*, probably due to a lack of this substrate near the active site of the enzyme.

Moreover, Fig. 2 presents a clear growth-phase dependency of the retinal content in *Synechocystis*. A higher retinal content was observed in the stationary phase for both WT and JBS14002 (each provided with pQC006). This could be a consequence of the fact that both *slr1648* and *sll1541* have a higher transcription level in the stationary phase than in the exponential phase (278), which would allow the cells to synthesize more retinal. Another possibility is that retinal is protected by PR from degradation during growth and accumulated to a high content in the stationary phase while simultaneously PR is slowly enzymatically degraded. Presumably, the C-terminal his-tag will be one of the first elements to be removed but the retinal binding pocket may withstand extensive proteolysis and keep its function (279), until eventually, the binding pocket will fall apart. This obliterates binding of the anti-his-tag antibody in Western blotting but could still allow stabilization of retinal against degradation, so that a large excess of retinal over intact proteorhodopsin could be present.

Furthermore, a higher retinal content in the stationary phase was observed in WT + pQC006 than in JBS14002 + pQC006, whereas the transcription level of *slr1648* reached a maximum under nitrogen deprivation conditions (278). We, therefore, consider it likely that *slr1648* significantly contributes to retinal synthesis in the late stages of growth because of the higher transcription level, induced by nitrogen deprivation. However, how SynDiox2 positively affects retinal production is still unclear. Possible explanations include supply or delivery of higher affinity or higher Vmax substrates to SynACO.

In addition, a pattern observed in both WT + pQC006 and JBS14002 + pQC006 shows that net retinal production of *Synechocystis* decreased slightly in the linear growth phase (*i.e.* at 58 h). Possibly, in this light-limited growth phase, carotenoids are directed towards the assembly of more photosynthetic machinery, thereby less flux of carotenoids is available for retinal synthesis.

Investigation of retinal degradation in *Synechocystis* is a delicate task, as retinal itself is chemically rather unstable. Our experiments on the stability of retinal in *Synechocystis* cultures have shown that its half- life is less than 2 hours. In addition, we found 10^4~10^5 molecules retinal per cell in WT + pQC006, but no retinal in WT cells, which implies that *Synechocystis* has the capability to efficiently synthesize and degrade (free) retinal. Moreover, deletion of related genes encoding presumed degradation enzymes did not lead to strong accumulation of retinal, which indicates the existence and a high capacity of a different mechanism, *i.e*. chemical- and multiple biochemical routes of degradation. Nevertheless, via the use of the expression of *apo*-PR, we observed that *slr0574* is involved in retinal degradation.

To determine the role of relevant genes in the retinal degradation pathway, a more straightforward approach would be to investigate the content and composition of retinoids (*i.e*. retinal, retinol and retinoic acid) separately among the various mutants and the WT. However, due to the instability of retinoids, complexity and overlap between different degradation mechanisms, quantitative estimation on retinoids is challenging. Instead, we propose to trace the fate of retinal in *vivo* in Synechocysits via supplementing [^{13}C] retinal into the culture. Preliminary results have been obtained by the degradation of 20 μM 3-[^{13}C] all-*trans* retinal degradation in a concentrated suspension (OD_{730} = 5) *Synechocystis* cells, harvested at the end of the linear phase of growth. Under those conditions, in a 24 h period, significant conversion of the retinal into retinol was observed (Q. Chen et al., unpublished observation). Neither the converse conversion, *i.e*. from retinol into retinal, nor from retinoic acid to retinal could be observed in wild type cells of *Synechocystis*, nor could any *holo*-PR be isolated from such incubations. The latter was also true for cultures of the SynACO deletion mutant JBS14001.

Another highlight of our study is that we show that a photo-active protein could be isolated from *Synechocystis* which can absorb light with wavelengths beyond 750 nm. While this protein has a low absorbance cross-section in the near infra-red, its pumping activity has been confirmed at 730 nm ((229)). Thereby, our work paves new ways to generate *Synechocystis* strains which

can exploit photons beyond 750 nm for (oxygenic) photosynthesis. This latter conclusion is reinforced by our recent observation that PR can also accelerate phototrophic growth in a PSI-deletion strain of *Synechocystis* (**chapter** 6).

Supplementary material:

Table S1: the primers used in this study

Name	Fragment [a]	Sequence [b]	Reference
JBS391	*sll1541* hom1 (F)	TACGAATTC CAATTGCGAGTAATT-AGAAGAAC	This study
JBS392	*sll1541* hom1 (R)	CTCCCGGCAT TCTAGA GGTCAAT-GGGGAAGTTTG	This study
JBS393	*sll1541* Ω (F)	ACTTCCCCATTGACC TCTAGA AT-GCCGGGAGTGTACAAAG	This study
JBS394	*sll1541* Ω (R)	CATCTAGACT ACTAGT CAAGC-GAGCTCGATATCC	This study
JBS395	*sll1541* hom2 (F)	TATCGAGCTCGCTTG ACTAGT AGTCTAGATGGCCACCGC	This study
JBS396	*sll1541* hom2 (R)	TACCTGCAG CTCAACAGCTTG-CCTTTGTTG	This study
JBS397	*slr1648* hom1 (F)	TACGAATTC CGGTG-GAAGATTTCATTC	This study
JBS398	*slr1648* hom1 (R)	GGGCATCGCG TCTAGA AGAGGG-GTGAAAAAATTTG	This study
JBS399	*slr1648* Cm (F)	TTTTTTCACCCCTCT TCTAGA CG-CGATGCCCTTTCGTCTTC	This study
JBS400	*slr1648* Cm (R)	GAAAATTTTC ACTAGT GATCGCG-CGATGGGTCGA	This study
JBS401	*slr1648* hom2 (F)	ACCCATCGCGCGATC ACTAGT GAAAATTTTCCGTCAGCATAG	This study
JBS402	*slr1648* hom2 (R)	TACCTGCAG CCTCCGGGAAACAA-CAAAG	This study
QC37	*slr0091* Ω (F)	ATTAACATT TCTAGA ATGCCGG-GAGTGTACAAAG	This study
QC38	*slr0091* Ω (R)	TGAATAATC ACTAGT CAAGC-GAGCTCGATATCC	This study
QC43	*slr0574* hom1 (F)	GAATTC CTTCTATTCGTGAG	This study
QC44	*slr0574* hom1 (R)	CGAAAGGGCATCGCG TCTAGA GGAAAGAAATAGGTTG	This study
QC47	*slr0574* hom2 (F)	ACCCATCGCGCGATCGCTAGC TTATTTGGTAGTGAAATTATTATTG-GC	This study
QC48	*slr0574* hom2 (R)	CTGCAG ATCGCTTCCGCC	This study
Adh-up-Fwd	*Slr0091* hom1 (F)	CAAGGAATTACTGGCATCTACC	This study
Adh-up-Rev	*Slr0091* hom1 (R)	GCCATAGGGAGAATAGCGTATCTA-GA GCTCAGCAACAACAGTTTTAG	This study
Adh-down-Fwd	*Slr0091* hom2 (F)	C T A A A A C T G T T G T T G C T - GAGCTCTAGA TACGCTATTCTC-CCTATGGC	This study
Adh-down-Rev	*Slr0091* hom2 (R)	GCGGTTTTGGTCACTCC	This study

[a] Ω is short for the omega resistance cassette; Cm for the chloramphenicol resistance cassette. Forward primers are indicated with (F); reverse primers with (R). [b] Sequences that overlap with the sequence of the target fragment are underlined. Sequences that overlap with the adjacent fragment for the fusion PCR are in italics.